



Experimental and numerical studies on the M-V-N interaction of longitudinally stiffened I-girders

André Biscaya¹, José O. Pedro², Ulrike Kuhlmann³

Abstract

In this paper we study the bending and shear interaction of compressed and longitudinally stiffened I-girders. Therefore, two full-scale tests were designed, and results are discussed. Moreover, to fill the gap in knowledge about imperfections in longitudinally stiffened girders, detailed information is given on initial geometric imperfections due to welding for the girder panels tested. Additionally, a finite element model is presented and verified against the experimental results. Following those outcomes, the resistance is compared against the effective width method and conclusions are drawn. These first results suggest the need for further investigation by numerical parametric analysis to analyze an improved design approach for the new version of the M-V-N interaction.

1. Introduction

In the past 50 years and following: (i) the development of construction technologies and (ii) societal demands, the use of cable-stayed bridges has been increasing and they are now widespread from medium to long spans (J. Pedro *et al*, 2016; H. Svensson, 2012). To be competitive, slender plates strengthened with transverse and longitudinal stiffeners are adopted in the design of bridge decks leading to complex buckling behaviors (J. Pedro, 2006; T. Lehnert, 2014). The design of cable-stayed bridge decks where slender plate girders are adopted presents a challenge, as they are suspended by the inclined stay cables which introduces high compression loads (R. Walther *et al*, 1999) as well as the typical bending and shear (M-V-N interaction). It is therefore required to understand their stability behavior when subjected to these combined loads. As consequence, these understanding favors optimized stiffening configurations and decreased steel quantities, promoting less onerous solutions (COMBRI, 2008; T. Lehnert *et al*, 2016).

Most of the studies in this field considered the bending-shear interaction (M-V interaction) without compression (Q.A. Hasan *et al*, 2017). In that regard, it is worth noting the recent works conducted by Sinur (F. Sinur *et al*, 2013; F. Sinur *et al*, 2013) and Jáger (B. Jáger *et al*, 2017; B. Jáger *et al*,

¹ PhD Student, CERIS, Instituto Superior Técnico, <andre.biscaya@tecnico.ulisboa.pt>

² Assistant Professor, CERIS, Instituto Superior Técnico, <jose.pedro@tecnico.ulisboa.pt>

³ Full Professor, Stuttgart University, <sekretariat@ke.uni-stuttgart.de>

2018) whom numerically and experimentally analyzed in depth a large range of stiffened and unstiffened I-girders.

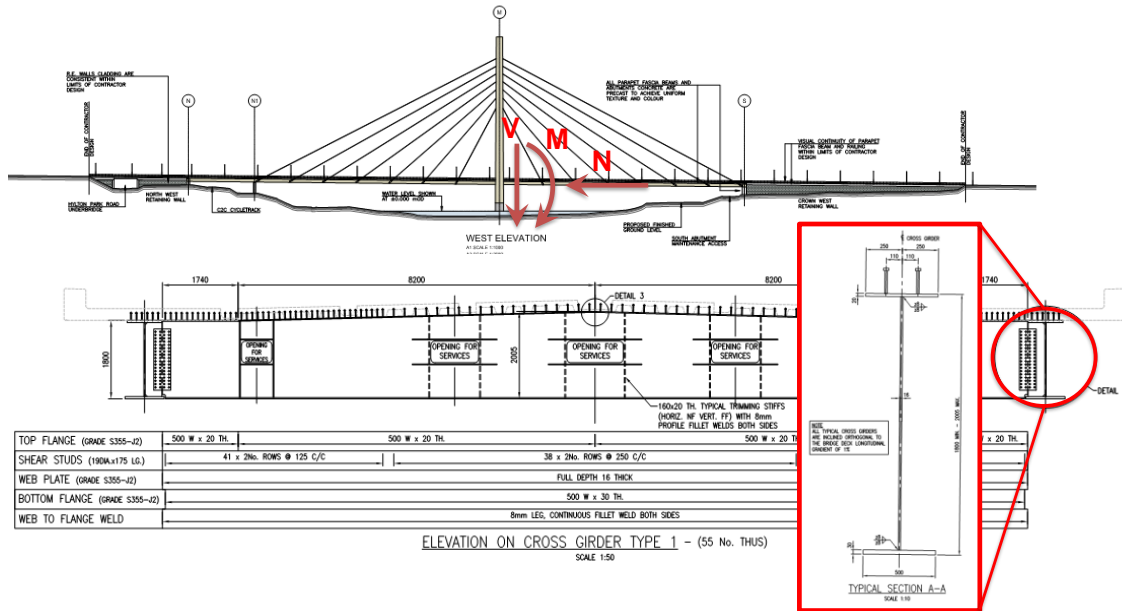


Fig. 1: Cable stayed bridge example and M-V-N interaction critical section.

Their work contributed to provide safe and reliable formulations applicable in the relevant range of shear and bending ratios in stiffened and unstiffened girders. These formulations were proven to be a better approximation of the real resistances than in current standards, such as the EN 1993-1-5 (CEN, 2006). On the other hand, presently the equations adopted in the EN 1993-1-5 are also applicable to the M-V-N interaction raising pertinent questions about the extensibility of the existing and recently proposed formulations when the compression is also taken into account.

While most research was carried out neglecting the influence of the axial compression to obtain the bending-shear interaction, only a few experiments were conducted to study its influence in steel plate girders (R.D. Ziemian, 2010). The test specimens from Horne (Horne *et al*, 1984) adopted unstiffened webs or one flat stiffener whereas the girders tested by Ogawa (H. Ogawa *et al*, 2016) - field of marine structures - were provided with multiple open stiffeners uniformly distributed along the web. Both the solutions adopted stiffeners with low torsional rigidity which is not favored in nowadays designs (B. Braun *et al*, 2009). Consequently, this work aims at fulfilling the gap in knowledge in the range of geometries analyzed and adds results adopting modern solutions with torsionally stiff closed stiffeners.

Following EN 1993-1-5 principles, the structural safety of steel plated girders with slender webs may be carried out in two possible ways: adopting (i) the effective width method (EWM) or the (ii) reduced stress method (RSM). Conceptually, while the first takes into account the whole cross-section, the former is based on a single plate slenderness. The EWM reduces the cross-section area considering the local buckling of the plate between stiffeners and global buckling of the stiffeners. As per the current European code, the interaction is checked with an interaction equation and depends on the compression level since it considers if the web is fully compressed or not.

Most recently, as per a new proposal under review within the CEN-TC250-SC3 (L. Dunai et al, 2018) the previous equations are replaced. It is worth noting that these equations were developed for M-V interaction and are extended hereafter to M-V-N interaction without any scientific background. Therefore, they only follow the same methodology as in the European code.

Moreover, the existing design equations have two branches depending on the compression levels and do not form a continuous and easy to use design method. This gap in knowledge was the driving force to undertake this research work.

2. Experimental investigations of plate girders under M-V-N interaction

2.1 General

In the frame of the testing program on the buckling behavior of longitudinally stiffened I-girders subjected to bending-shear-compression interaction, tests have been conducted on two welded plate girders. The tests were prepared with the purpose of studying the influence of the compression applied to the girders under interaction of bending moment and shear force. Therefore, they differ in one isolated parameter to analyze the effect on the buckling resistance and validate the finite element model used.

The tests parameters were obtained based on numerical calculations and maximum jack load limited to 2500 kN. The preliminary design was based on the effective width method in the domain where the interaction between bending, shear and compression was expected.

2.2 Test Girders

Two simply supported I-girders with 4750 mm span subjected to mid-span point loading and different levels of compression force, namely GL (Girder Low) and GH (Girder High), were studied. The flanges, web, transversal stiffeners and length of test panels remained the same for all the tests.

The parameters of the tested panels are shown in Fig. 2 and the geometry of the tested panels are summarized in Table 1 and 2.

Both girders are double-symmetric and transverse stiffeners have the same width and thickness as the flanges that are designed to comply with limits of class 2. Both flanges are laterally braced at mid-span and supports. The web is designed to have typical geometric slenderness of $h_w/t_w = 185$ and aspect ratio of $a/h = 1.5$ to follow typical cable-stayed bridge ratios, having strong torsional buckling longitudinal stiffeners with closed cross-section. In addition, the b_{si}/t_s ratios of the longitudinal stiffener walls components should comply with the limits of class 3 sections to avoid premature buckling. Thus, closed-section trapezoidal stiffeners were considered with relative bending stiffness $\gamma = 50 > 25$ to fulfil strong stiffness requirements and to have higher rigidity than the minimum stiffness's which prevents pure compression and bending global buckling, although lower than the minimum stiffness which prevents pure shear global buckling when 1 or 2 stiffeners are used $\gamma_{1s}^* = 140$ and $\gamma_{2s}^* = 167$, respectively.

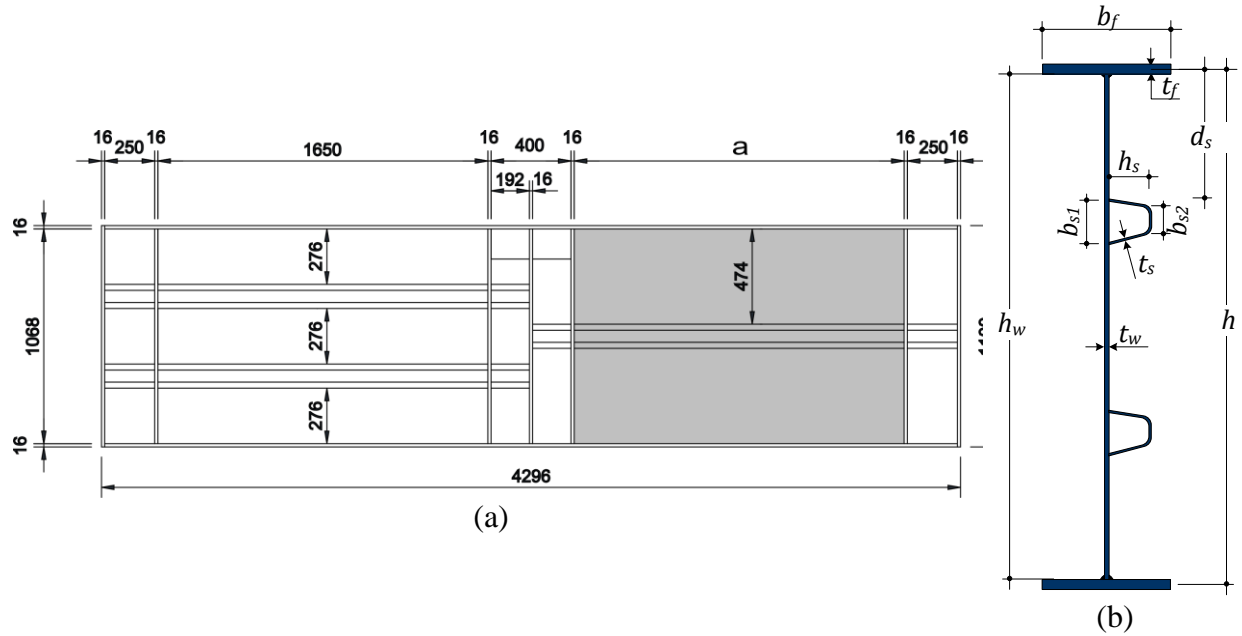


Fig. 2: Test Girder: (a) Panel dimensions and (b) Geometry of cross section.

Table 1: Dimensions of the tested panels and tests.

Tested Panel	N_{test} [kN]	a [mm]	h_w [mm]	t_w [mm]	b_f [mm]	t_f [mm]	Stiffener
GL_1S	1250	1650	1068	6	300	16	1 stiffener
GH_1S	2000	1650	1068	6	300	16	1 stiffener

Table 2: Stiffener dimensions.

Tested Panel	h_s [mm]	t_s [mm]	b_{s1} [mm]	b_{s2} [mm]	d_s [mm]
GL_1S	70	4	120	16	482
GH_1S	70	4	120	16	482

2.3 Material of test girders

The assessment of the steel properties was carried out by tensile coupon tests according to ISO 6892-1 and the coupon were taken from the plates used to fabricate the girders. Fig. 3 shows the average stress-strain relations calculated from tests (three per plate thickness) and Table 3 shows the corresponding yield strength f_y , ultimate strength f_u and ultimate strain ϵ_u . For the purpose of numerical simulations, the measured curve was broken into a 5-linear curve.

Table 3: Mechanical properties of the steel coupons.

Plate	f_y [MPa]	f_u [MPa]	ϵ_u [%]
Stiffener - 4 mm	450	535	18
Web - 6 mm	344	460	24
Flange - 16 mm	335	471	30

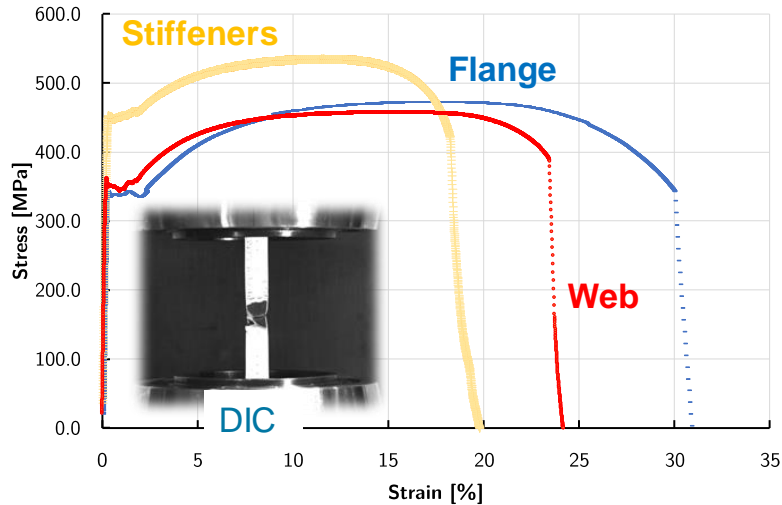


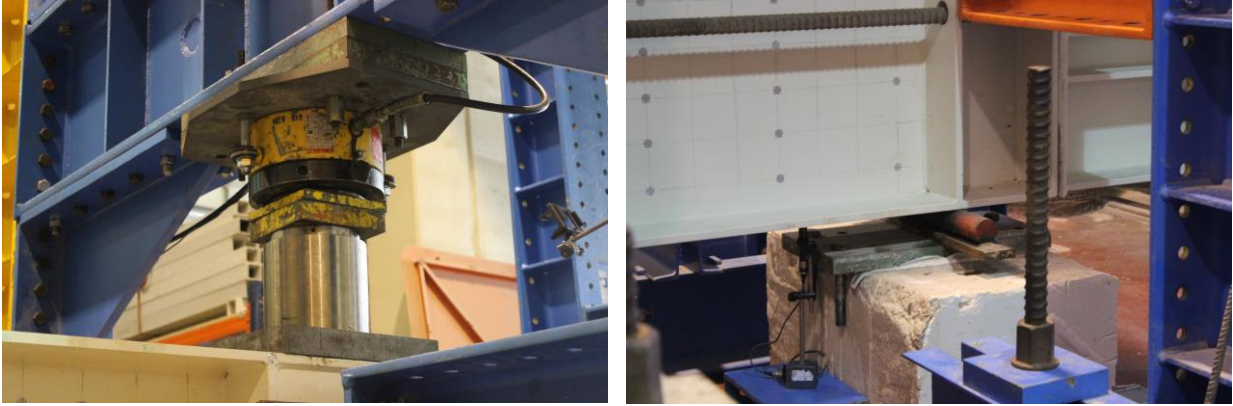
Fig. 3: Stress-strain curves gathered from the tensile tests of the coupons.

2.4 Test setup and procedure

The girder tests were performed using the setup shown in Fig. 4. The setup consisted of one large portal frame at the beam mid-span and two lateral frames at the supports providing the necessary bracing to avoid lateral flange displacements. All the three frames were longitudinally braced with an HEA 600 beam. The central frame included the ENERPAC hydraulic jack, with a capacity of 250 tons and 50 mm maximum course. The stamp of the hydraulic jack received a calotte in order to apply the load always in the vertical direction and to mitigate any horizontal restraining forces (Fig. 5 (a)). All the portal frames were tied to the ground slab with 36 mm Dywidag prestressed bars in order to avoid any uplift of the testing rig.



Fig. 4: Test setup.



(a) (b)
Fig. 5: Testing rig equipment's: (a) hydraulic jack and (b) supports.

We adopted steel cylinders to allow rotations at the supports. These elements were installed on top of a steel plate and concrete blocks to spread the load transferred to the ground (Fig. 5 (b)).

In order to carry out the experimental tests it was necessary to define the levels of compression for the GH and GL cases. Two possible candidates were: (i) GH - when all the web in compression; and (ii) GL - when the girder is subjected to some level of compression, but the web show tensile stresses. Accordingly, Table 4 shows a set of compression forces deemed to satisfy these requirements.

Table 4: Levels of compression.

test	$N_{\text{test}}/N_{\text{eff.Rd}}$ [%]	ψ [-]	% F_{puk} [%]
GL_1S	26.1	-0.50	30
GH_1S	41.7	0	48



(a) (b)
Fig. 6: Compression bars: (a) elevation and (b) anchorage.

These forces were applied with four prestressing bars ($F_{puk}=1050$ kN) anchored on HEB500 spreader beams, two either side of the web and located to match the elastic neutral axis hence avoiding stress losses due to girder bending (Fig. 6). The compression load is fully applied before the girder is vertically loaded and kept constant during the test.

2.5 Geometric imperfections due to welding

Out-of-plane web deflections were measured with laser method. The panel surface was marked with reflecting targets to be able to clearly follow the deformation of a specific point along the testing (Fig. 7).



Fig. 7: Geometric imperfection measure.

It is shown on Fig. 8 the out-of-plane web imperfection for girder GL_1S where it is visible the global dominance from the longitudinal stiffener bow imperfection with 3.5 mm amplitude. It is worth to note the existing imperfection along the borders between the web and flanges generally not taken into account in codified equivalent imperfection patterns. The measurements for GH were similar and are not shown for brevity. This amplitude represents 63 % of the amplitude preconized in the European code for GMNIA analysis and were therefore within tolerance.

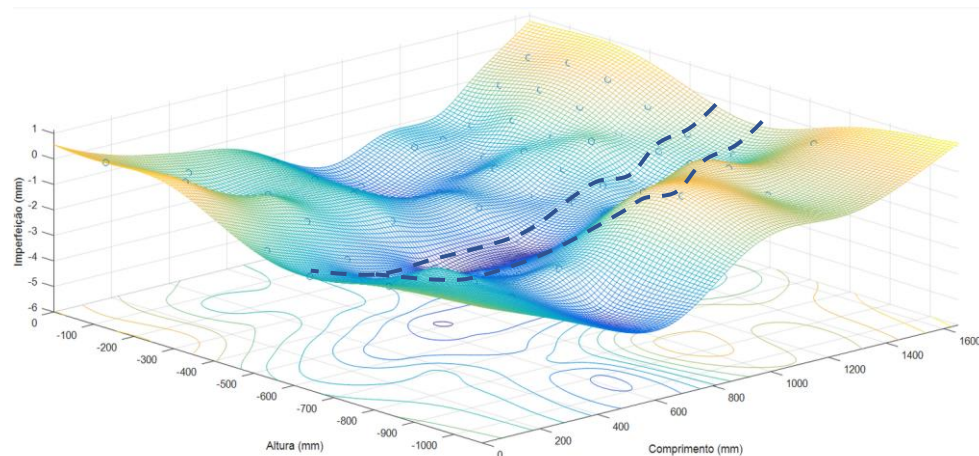


Fig. 8: Geometric imperfection measurement.

Residual stresses due to welding were not measured since they have little influence on the behavior in shear dominated problems of the web.

2.6 Test Results

The load-displacement curves for all girders are shown in Fig. 9 (a) and (b). The higher resistance was obtained for GL_1S in which the compression load is lower. Both girders showed a linear elastic response up to a high load level. As they cross over to the plastic domain, the stiffness gradually decreases until they reach the maximum load capacity. After that point, the load decreases. The displacement for the maximum load being reached is lower in the test with high compression force, around 45% less.

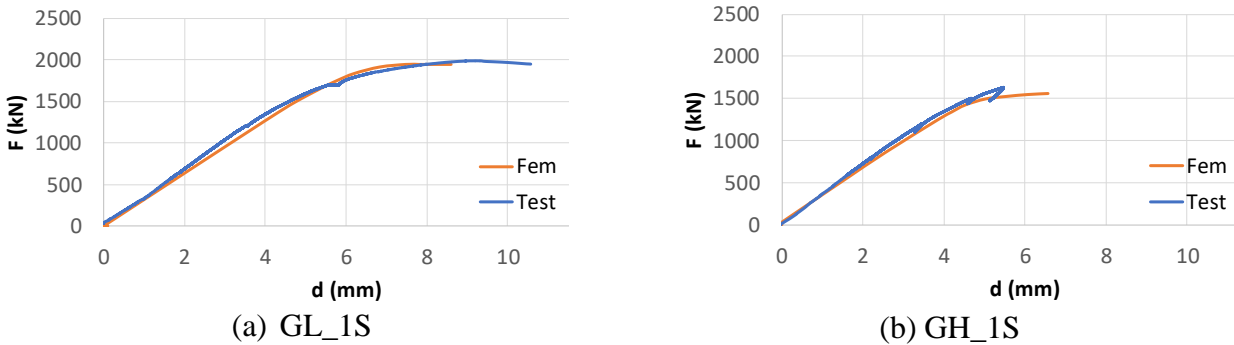


Fig. 9: Load-displacement curve: (a) GL_1S and (b) GH_1S.

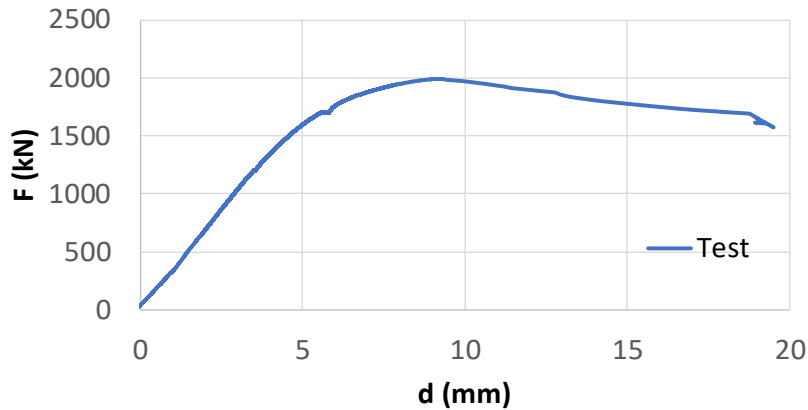


Fig. 10: GL_1S complete load-displacement curve.

At the maximum load both girders have buckled webs on the top panel near to the mid-span, as shown in Fig. 11. The collapse deformations prompt the following comments:

- Increasing the compression load leads to less inclined buckling half-waves, almost the same as in pure axial stress buckling shape;
- After the peak being reached, the GL_1S test showed a gradual decrease in load until losing the load carrying capacity at 18 mm displacement (Fig. 10). However, at that time an instantaneous drop of capacity due to column-like instability of the longitudinal stiffener occurred (Fig. 12 (a)). Therefore, the girder rotational capacity is quite limited;

- The described behavior was due to the stress shedding occurring at the top web panel with compressions migrating from the web to the longitudinal stiffener and leading to that type of instability quite unexpected;
- The shape of the column-like buckling is similar to a double half-wave and follows the measured imperfection pattern as shown in Fig. 12 (b).
- In regards to the GH_1S test and since the damage from that collapse type is high, it has been decided not to go as far in displacements after peak load;



Fig. 11: Out of plane displacements: (a) GL_1S and (b) GH_1S.

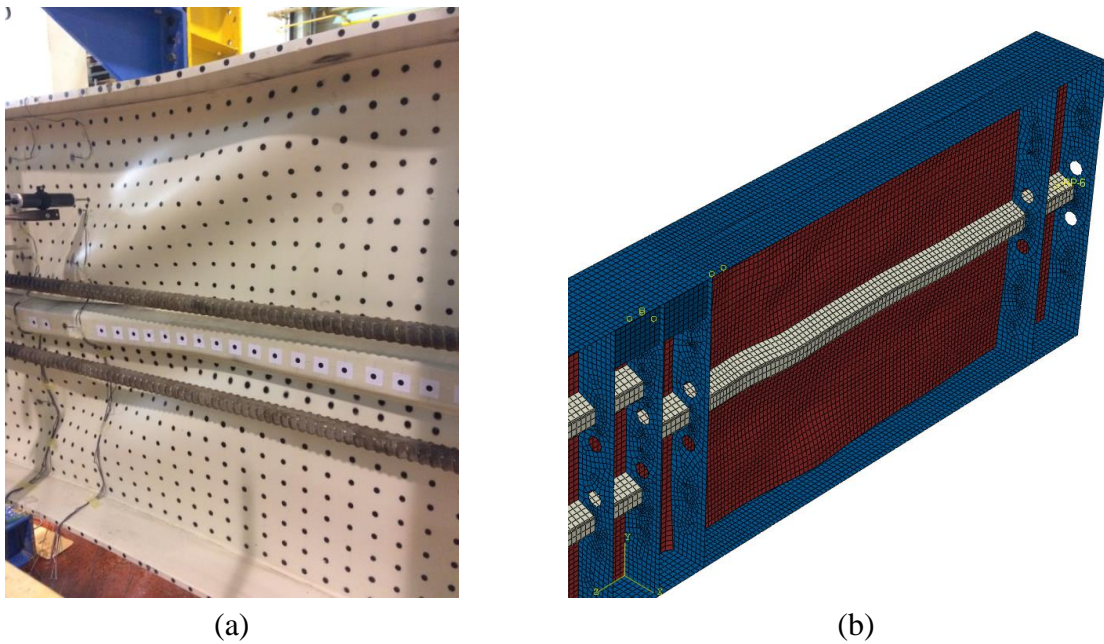


Fig. 12: Out of plane displacements: (a) Column-like buckling and (b) imperfection shape.

- A very good agreement was found between the numerical simulations and test results as shown in the next section.

3. Numerical investigations

3.1 Numerical model

Girders ultimate capacity was assessed with GMNIA analysis using ABAQUS software [8]. Material elasto-plastic behaviour was considered using measured stress-strain curves, Young's modulus $E = 210 \text{ kN/mm}^2$. Analysis was undertaken using the RIKS method and S4R shell elements of 25 mm size were utilized. As example, Fig. 13 shows the imperfection shape imported to Abaqus via Python scripting.



Fig. 13: Finite element model with geometric imperfection.

The vertical supports were set along the bottom edge of both inner end-post stiffeners. The longitudinal displacement was restrained at the position of vertical load application. This load was applied by a rigid body representing the plate between the loading cell and the girder. The lateral supports were modelled as rigid at the same positions as per the experimental tests.

3.2 FEM Results

In Fig. 9 the load-displacement curve is compared against the numerical solution. They show a very good agreement both in displacement as well as load. In Table 5 the maximum load carrying capacities from the test and FEM are compared. The differences range from 2.4% to 4.7% which is considered almost neglectable.

Table 5: Comparison between numerical and test.

Test	N_{exp} kN	$N_{exp}/N_{eff,rk}$ %	F_{exp} kN	F_{num} kN	Dif %
GL_1S	1250	26.1%	1991	1945	2.4%
GH_1S	2000	41.7%	1631	1558	4.7%

For the numerical simulations the same type of local buckling occurred.

4. Comparison with recently proposed interaction formulae

In order to compare the test results to code provisions, the characteristic resistance was calculated using the effective width method. Both the shear and bending capacities are calculated separately and the bending is linearly reduced by the compression load (see Fig. 14).

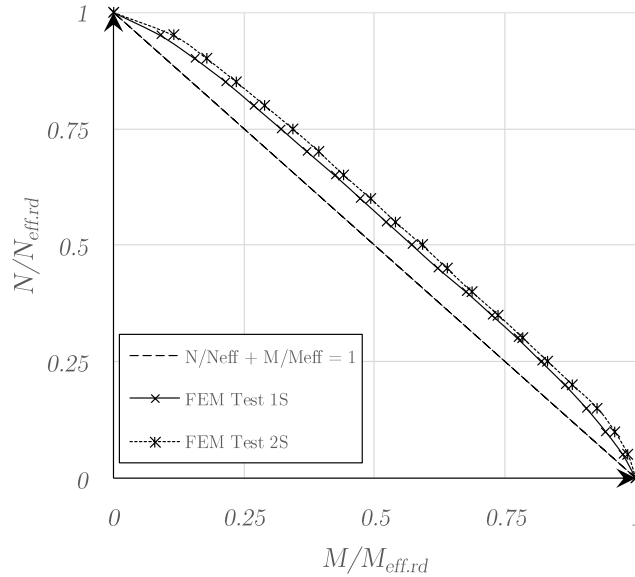


Fig. 14: M-N interaction.

Comparing the results, it can be depicted from Fig. 15 that the test results almost matches the proposed interaction curve when the branch between the effective bending moment and the flange bending moment is taken as straight ($\beta=1$).

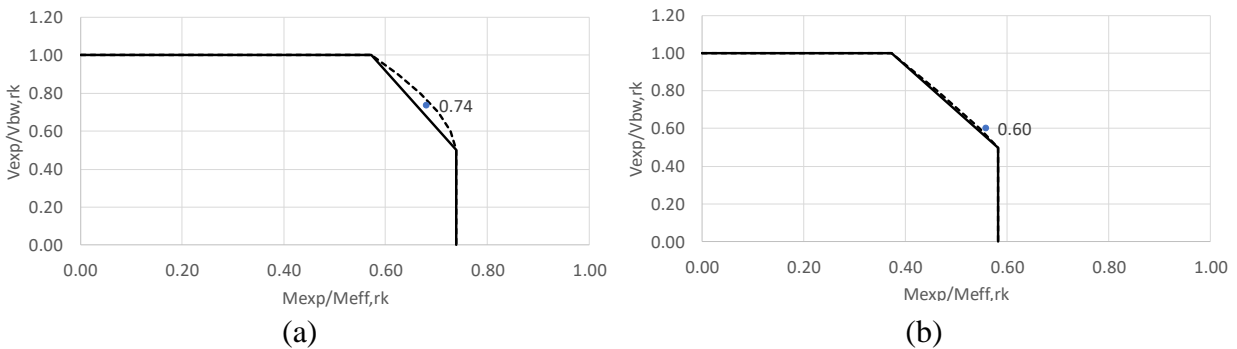


Fig. 15: Comparison between test result (blue dot) and recently proposed European formulae.

5. Conclusions

Experimental investigations have been conducted on two welded girders. The tests focused explicitly on the influence of the compression load on the M-V interaction. A good agreement between tests and numerical simulation was attained.

It is shown experimentally the reasonability of using the recently proposed formulation with $\beta=1$ for the M-V-N interaction in the compression range tested.

In following steps, tests with two web stiffeners are carried out and a numerical parametric study will be performed to cover different configurations. Then the recently proposed rule will be evaluated and enhanced also based on a statistical approach.

Acknowledgments

The first authors of this paper gratefully acknowledge the financial support provided by the grant SFRH/BD/116316/2016.

References

- B. Jáger, B. Kövesdi, L. Dunai (2017) *I-girders with unstiffened slender webs subjected by bending and shear interaction*, J. Constr. Steel Res. 131, 176–188.
- B. Jáger, B. Kövesdi, L. Dunai (2018) *Bending and shear buckling interaction behaviour of I-girders with longitudinally stiffened webs*, J. Constr. Steel Res. 145, 504–517.
- B. Braun, Kuhlmann U. (2009) *Bemessung und Konstruktion von aus Blechen zusammengesetzten Bauteilen nach DIN EN 1993-1-5*, Stahlbau-Kalender, Verlag Ernst & Sohn; p. 381–453.
- CEN (Comité Européen de Normalisation) (2006). *Eurocode 3: Design of Steel Structures - Part 1-5: Plated Structural Elements*, EN 1993-1-5:2006, Brussels, Belgium.
- COMBRI (2008) *COMBRI DESIGN MANUAL Part II: State-of-the-Art and Conceptual Design of Steel and Composite Bridges*, RFCS.
- F. Sinur (2011) *Behaviour of longitudinally stiffened plate girders subjected to bending-shear interaction*, University of Ljubljana, PhD Thesis.
- F. Sinur, D. Beg (2013) *Moment-shear interaction of stiffened plate girders - Numerical study and reliability analysis*, J. Constr. Steel Res. 88, 231–243.
- H. Svensson (2012) *Cable-stayed bridges - 40 Years of Experience Worldwide*, Wiley.
- H. Ogawa, T. Takami, A. Tatsumi, Y. Tanaka, S. Hirakawa, M. Fujikubo (2016) *Buckling/Ultimate Strength Evaluation for Continuous Stiffened Panel Under Combined Shear and Thrust*, ASME 2016 35th International Conference on Ocean, Offshore and Arctic Engineering, 1–9.
- J. Joaquim (2007) *Pontes atirantadas mistas - Estudo do Comportamento Estrutural (in portuguese)*, IST, MSc Thesis.
- J. Joaquim, A. Reis (2016) *Composite cable-stayed bridges: state of the art*, Proceedings of the Institution of Civil Engineers - Bridge Engineering, n. 169.
- L. Dunai (2018), *Cen/tc 250/sc 3 n 2496*, ECCS.
- M. Horne, W.R. Grayson (1984) *Ultimate load behavior of stiffened web panels subjected to combined stress*, Proceedings of the Institution of Civil Engineers, 635–656.
- Q.A. Hasan, W.H.W. Badaruzzaman, A.W. Al-zand, A.A. Mutalib (2017) *Thin-Walled Structures The state of the art of steel and steel concrete composite straight plate girder bridges*, Thin Walled Struct. 119, 988–1020.
- R. Walther (1999) *Cable-stayed bridges*, Thomas Telford
- R. Ziemian (2010), *Guide To Stability Design Criteria for Metal Structures*, 6th ed., John Wiley & Sons, Inc.
- T. Lehnert, F. Schröter (2014) *How Modern Steel Developments Can Help Optimizing Cost and Sustainability of Bridge Constructions*, Dillinger
- T. Lehnert, F. Schröter (2016) *Recent developments in heavy plate production for modern steel bridges*, Recent Prog. Steel Compos. Struct. - Proc. 13th Int. Conf. Met. Struct. ICMS, 331–336.